International Journal of Innovations in Engineering and Technology (IJIET)
http://dx.doi.org/10.21172/ijiet.241.01

Influence of Stress Triaxiality on Tensile Properties at Cryogenic Temperature in Mg-3Al-1Zn Alloy

Akihiro Takahashi
Department of Mechanical Engineering
National Institute of Technology (KOSEN), Miyakonojo College, Miyakonojo, Miyazaki 885-8567, Japan

Natsuki Takagi
Department of Mechanical Engineering
National Institute of Technology (KOSEN), Miyakonojo College, Miyakonojo, Miyazaki 885-8567, Japan

Toshinobu Toyohiro
Department of Mechanical Engineering
National Institute of Technology (KOSEN), Miyakonojo College, Miyakonojo, Miyazaki 885-8567, Japan

Abstract- This paper experimentally investigates the influence of stress triaxiality values from 0.3 to 1.4 on cryogenic tensile properties and fracture behavior in a wrought AZ31 magnesium (Mg) alloy fabricated by hot extrusion. Round bar specimens consisting of four gradients of notch-root-radii and smooth round bar specimens were examined at room temperature and 83 K, respectively. Ductility at cryogenic temperatures was drastically lower than that at room temperature. Fractography techniques were employed to interpret SEM observations. Three fracture behaviors were identified. Issues were also identified with the application of the Rice and Tracy model to the fracture behavior in AZ31Mg alloy under cryogenic temperatures. Thus, the use of Mg alloys for structural materials at cryogenic temperatures is a serious issue, and must be addressed in applications employing these materials to avoid unnecessary risks.

Keywords – magnesium alloy, stress triaxiality, tensile property, cryogenic temperature, fracture surface

I. INTORODUCTION

Magnesium (Mg) alloys possess a density relative to steel of 22 %, and 63 % that of aluminum alloys with the strength-to-weight ratio of Mg alloys far exceeding other metallic materials. These alloys are attractive structural materials to minimize weight. For this reason, Mg alloys are used for not only automobile and aerospace applications, but also many other applications, such as sports goods, electronic components, telecommunication devices, and biomaterials, due to performance optimization through multi-material design [1]. The quality of the mechanical structure dictates material responses to stress distribution during loading. Stress distribution influenced by microstructure, initial defects, configuration and dimensions, and thermal history in weldment all influence plastic deformation and damage progression within structural materials. Stress triaxiality is a quantitative value to evaluate the stress distribution and behavior, and is an important metric for structural materials in understanding the processes from initial deformation to ductile fracture [2]. The relationship between plastic ductility and stress triaxiality in metallic materials is often investigated with notched tensile specimens [3-5]. Ductile fracture research using notched round bar specimens with various notch-root-radii for AZ31Mg alloys was investigated by Kondori and Benzerga [6] and for Mg-Al-Zn-RE alloy by Li and Fang [7]. They reported that room temperature (RT) ductility decreased with an increase in stress triaxiality. However, there are no reports of the relationship between tensile properties and stress triaxiality under cryogenic conditions. This analysis is important as high-risk applications such as storage and transport of LNG requires temperatures below 100 K and would benefit from light-weight alloys. As Mg alloys are lightweight and strong, they are excellent potential structural materials for fuel transportation. Therefore, investigation of the interplay of stress triaxiality on tensile properties and fracture characteristics in Mg alloys under cryogenic conditions is necessary to develop new materials for improved fuel-efficiency and to provide clearer design guidelines and improved production techniques for materials requiring low-temperature resistance.

The present study explores the influence of stress triaxiality on tensile properties, plastic strain until break point, and failure mode at RT and 83 K for AZ31Mg alloy notched round bar specimens.

II. EXPERIMENTAL PROCEDURE

Commercial hot-extruded AZ31Mg alloy was used as the starting material. Table 1 shows the material chemical composition. Fig. 1 shows the microstructures observed along the extrusion direction of the material. The average grain size and hardness are 12.5 μm and 58 HV.

A smooth round bar and several notched round bar specimens for tensile test were machined from the as-received material along the extrusion direction.

Table 1. Chemical composition of the AZ31Mg alloy used in this study

Al	Zn	Mn	Si	Fe	Cu	Mg
2.98	0.93	0.38	0.01	≦0.001	≦0.001	Bal.

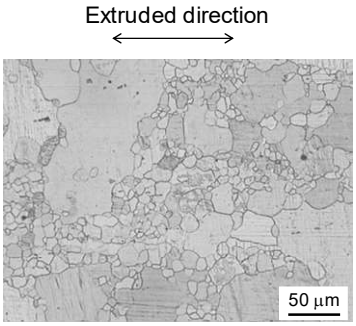

Figure 1. Optical micrograph of the AZ31Mg alloy used in this study.

Stress triaxiality based on Bridgeman's equation [8] is given by Eq. (1).

$$\frac{\sigma_m}{\bar{\sigma}} = \frac{1}{3} + In\left(1 + \frac{a}{2R}\right) \quad (1)$$

where σ_m is the mean stress, $\bar{\sigma}$ is the Von-Mises's equivalent stress, a is the ligament (lateral diameter), and R refers to the notch-root-radius (adopting R = 1, 3, 6 and 12 mm). In the smooth specimen, R tends to infinity, leading to a stress triaxiality of 0.33 by employing Eq. (1). Specimen configuration and dimensions are illustrated in Fig. 2. Unload-reloading tensile tests were carried out on a SHIMADZU universal machine with load capacity of 50kN at an initial loading speed of 1 mm/min at room temperature and 83 K. True stress, σ, can be described by $\sigma = P/A$, where P is applied load and A is true area calculated from the result of lateral deformation between notch roots during tension. True strain (i.e., equivalent plastic strain), $\bar{\varepsilon}_p$ is written by $\bar{\varepsilon}_p = 2ln(d_0/d)$,

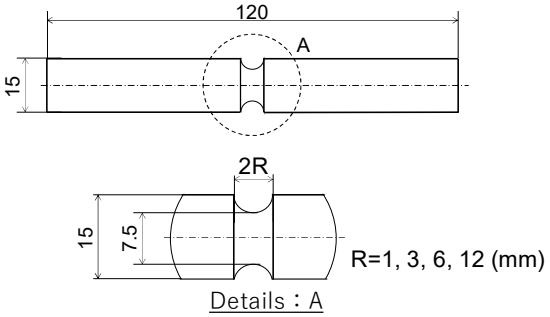

(a) Notched round bar specimen

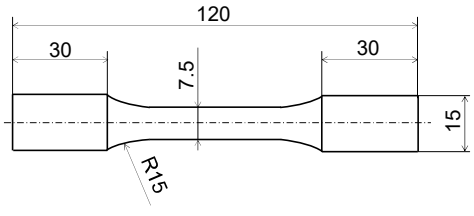

(b) Smooth round bar specimen

Figure 2. Configuration and dimensions of the AZ31Mg alloy test specimens.

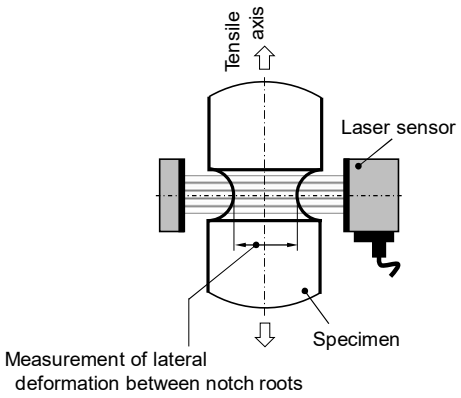

Figure 3. Ligament value measurement by a transmission type laser sensor during tensile test.

where d_0 is the ligament value before tensile test and d is the ligament after specimen deformation. The ligament deformation at the lower section of the notch was measured by a transmission type laser sensor (accuracy better than 0.005 mm) as shown in Fig. 3. Critical plastic strain, $\bar{\varepsilon}_f$, at the specimen breaking point is represented by $\bar{\varepsilon}_f = 2ln(d_0/d_f)$, where d_f is the fractured ligament value measured by caliper.

Tensile testing under cryogenic conditions was performed using liquid nitrogen as the coolant. The test specimen was surrounded with foam blocks, and the sample cooled using a moderate stream of liquid nitrogen directly blown on the specimen, enabling the cryogenic tensile testing at 83 K. Temperatures during cryogenic testing were measured using a thermocouple placed adjacent to the test specimen. To suppress frost formation on the test specimen surface, before testing, the notch-root region was coated with organic wax. In this cryogenic test, while temporarily suspending the test, the ligament diameter, d, was measured over several seconds by a laser sensor. After diameter measurement, the test was restarted once the temperature stabilized at 83 K.

SEM was used to observe the entire specimen fracture surface at the testing temperatures of RT and 83 K.

III. RESULTS AND DISCUSSIONS

3.1. True stress-true strain curve –

Fig. 4 shows the typical true stress-true strain curves of AZ31Mg with different notch-root-radii at RT. The R value is observed to decrease with increased yield stress and tensile strength. Conversely, ductility decreased with an increase in R value. Progressively, tensile fracture was confirmed at the maximum load point in all specimens. This demonstrates that the R value is closely related to the plastic constraint within the range of stress triaxiality.

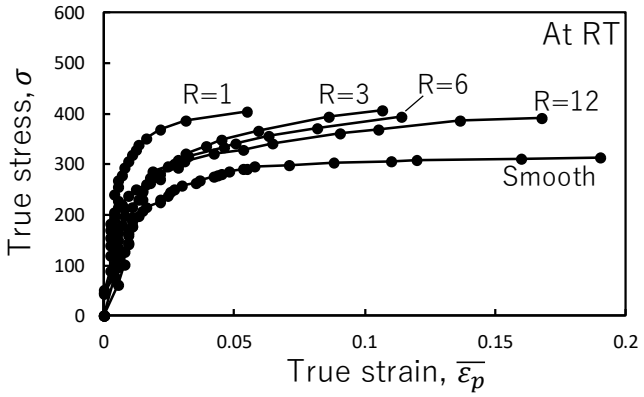

Figure 4. True stress-true strain curves of the specimens tested at RT.

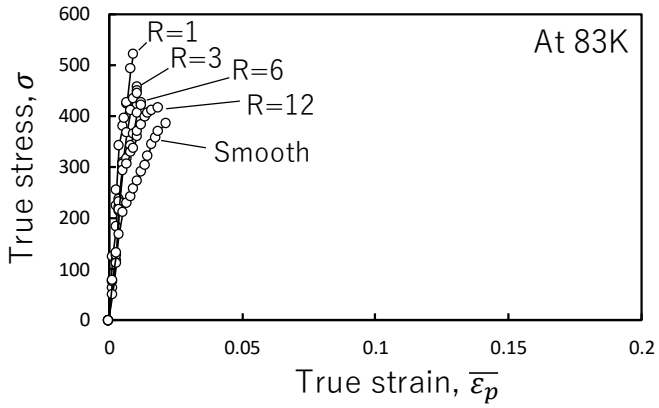

Figure 5. True stress-true strain curves of the specimens tested at 83 K.

Fig. 5 shows the typical true stress-true strain curves tested at 83 K. A tendency towards large decreases in cryogenic ductility (i.e., critical plastic strain, $\bar{\varepsilon}_f$) were observed. For example, ductility at 83 K decreased by 13 % for the smooth specimen and 24 % for the R = 1 specimen compared to RT. On the other hand, tensile strength at 83 K increased by 23 % for the smooth specimen and 19 % for the R = 1 specimen compared to RT. This demonstrates the brittle behavior of Mg alloys under cryogenic temperatures.

3.2 Stress triaxiality and critical plastic strain –

Fig. 6 shows the relationship between critical plastic strain, $\bar{\varepsilon}_f$, and stress triaxiality, $\sigma_m/\bar{\sigma}$. At RT, the critical plastic strain decreased with increased stress triaxiality. At 83 K, the critical plastic strain was greatly reduced independent of stress triaxiality. Zheng et al. [9] conducted tensile testing of pure Mg with grain size of 18 μm at RT and 77 K, reporting a 31 % reduction in tensile ductility at 77 K from RT, concluding that Mg ductility was insensitive to testing temperature. Takahashi et al. [10] evaluated the AZ61Mg alloy, reporting that impact energies at cryogenic temperatures of 83 K showed degradation of approximately 55 % compared to that at RT. Also noting that the fracture morphology at 83 K represented a brittle fracture surface. The decrease of cryogenic tensile ductility observed in present study agrees well with the reports of Zheng and Takahashi.

3.3 Fracture behavior –

Fractography was carried out by SEM with typical photographs at RT and 83 K displayed in Figs. 7 and 8. The micrograph in Fig. 7 (a) displays the smooth specimen fracture surface tested at RT. The micrograph reveals a fracture mode characterized by shallow dimple failure, indicating substantial ductility. This may be attributed to the influence of microstructural texture and the arrangement of second phase particles, particularly those associated with the Al-Mn system in the Mn-rich region and the β-$Mg_{17}Al_{12}$ intermetallic phase. Increasingly, split-type

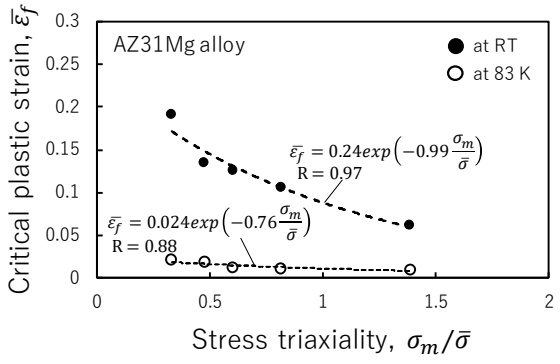

Figure 6. Critical plastic strain as a function of stress triaxiality.

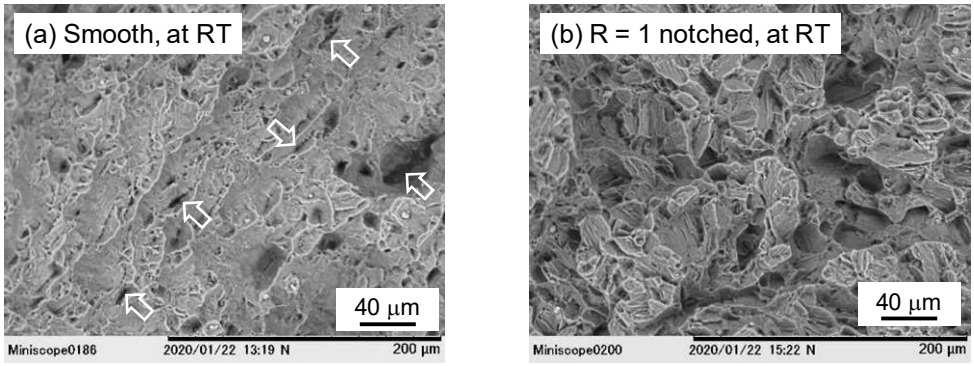

Figure 7. Tensile fracture surfaces of the (a) smooth specimen and (b) R = 1 notched specimen tested at RT.

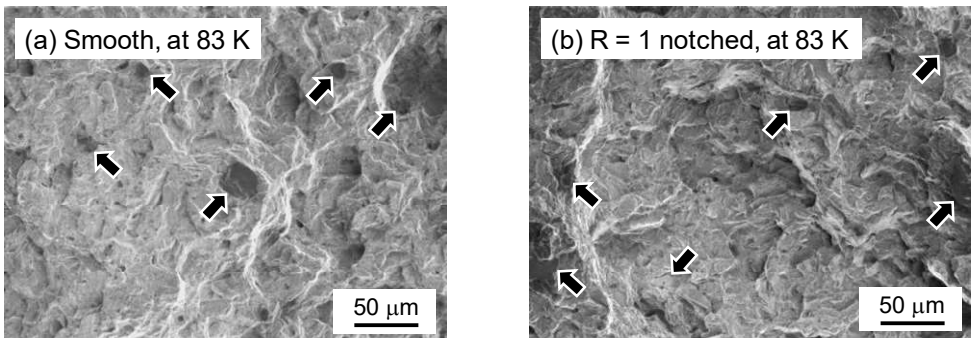

Figure 8. Tensile fracture surfaces of the (a) smooth specimen and (b) R = 1 notched specimen tested at 83 K.

cracks and second phase particles into a few dimple bottoms are also observed. Arrows in Fig. 7 (a) indicate the split-type cracks. Li and Fang [7] demonstrated that these cracks originate from twin-induced and particle-induced micro-defects. Fig. 7 (b) displays the fracture surface of a notched specimen (R = 1) tested at RT. The surface appears to be mostly ruggedly fractured with cleavage facets, compared to the smooth specimen surface. The absence of cleavage facets is likely due to the suppression of deformation twinning. The number of dimples in notched specimen (R =1) is less than that for the smooth specimen. Moreover, the intergranular fracture surface is dominant in the micrograph, strongly indicating that the fracture strain (i.e., critical plastic strain) in notched specimens is lower than that for the smooth specimen.

Fig. 8 (a) and (b) show fracture surfaces of the smooth specimen and R = 1 notched specimen tested at 83 K. The fracture surfaces are markedly different between 83 K and RT. At the lower temperature, the dimple failure is not prevalent, instead displaying numerous brittle fractures of coarse rounded particles greater than 10 μm in diameter (Fig. 8 (a)). These particles appear to be coarse second phase particles comprised of Al-Mn and Mg-Al components. Brittle fracture of second phase particles is also evident in Fig. 8 (b). Furthermore, a degree of rugged fracture mode occurs in comparison to Fig. 8 (a). Given the increased embrittlement of coarse second-phase particles that emerge, even under different stress states, the particle fracture strength appears extremely low under cryogenic temperatures. Consequently, a low tensile ductility is observed with the fracture surfaces exhibiting cleavage fractures.

As previous local models described the process of void growth in terms of void initiation due to cracking and interfacial debonding with second phase particles, McClintock [11] analyzed the growth of a cylindrical void in a rigid plastic body under axisymmetric loading. Rice and Tracy [12] proposed an approximate solution for spherical void initiation and growth. Then a model analyzing plastic flow in a porous metal based on Rice and Tracy's methodology was developed by Gurson [13]. Subsequently, the GNT (Gurson- Needleman - Tvergaard) model was proposed, improving and redefining the function of void volume fraction from the Gurson model [14, 15]. This

model and its variations are reported by many researchers [16-18]. Kobayashi et. al. [19-22] also analyzed ductile fracture behavior in several structural metallic materials based on the spherical void growth model by Rice and Tracy [12]. The Rice and Tracy model is given by Eq. (2)

$$\frac{dR_V}{R_V} = ad\bar{\varepsilon}_p exp\left(b\frac{\sigma_m}{\bar{\sigma}}\right) \quad (2)$$

where R_v is the radius of the void. $d\bar{\varepsilon}_p$ is the increment of equivalent plastic strain. With a and b as material constants. Eq. (2) is integrated, and then it is given as follows,

$$In\left(\frac{R_v}{R_{v0}}\right) = a\bar{\varepsilon}_p exp\left(b\frac{\sigma_m}{\bar{\sigma}}\right) \quad (3)$$

where R_{v0} is the initial radius of the void. Assuming that the critical void radius at ductile crack initiation is constant, the left-part of Eq. (3) can be regarded as a constant. Thus,

$$\bar{\varepsilon}_f = a' exp\left(-b'\frac{\sigma_m}{\bar{\sigma}}\right) \quad (4)$$

where the a' and b' are material constants. Dashed lines in Fig. 6 represent a plot of Eq. (4). At RT, the constants are a' = 0.24, b'=0.99, with a correlation coefficient of R = 0.97. However, at 83 K, a' = 0.024, b'=0.76, with a correlation coefficient of R = 0.88, seen in Fig. 6. The a' value represents critical plastic strain sensitivity to stress triaxiality. Thus, as a' at cryogenic temperatures is lower than that at RT, it is concluded that the critical plastic strain is insensitive to stress triaxiality. However, it is necessary to further discuss application of the Rice and Tracy model [12] to fracture behavior in Mg alloys at cryogenic temperatures, as different plastic deformation and fracture processes occur. Regardless, the critical plastic strain in AZ31Mg alloy at cryogenic temperatures is extremely low, and improvement of cryogenic plastic strain properties is still required.

IV.CONCLUSION

To investigate the relationship between tensile property and stress triaxiality under cryogenic temperatures, a tensile test with notched round bar specimens was carried out with static loading speed of 1 mm/min at a testing temperature of 83 K. Fractography by SEM was also performed to evaluate fracture behavior relating to the mechanical properties at both temperatures. The results are summarized as follows:

1. At room temperature, critical plastic strain, $\bar{\varepsilon}_f$ decreased with increasing stress triaxiality. $\bar{\varepsilon}_f$ of the smooth round bar specimen tested at 83 K was 13 % less than that at room temperature. On the other hand, $\bar{\varepsilon}_f$ of notched round bar specimen with notch-root-radius of R = 1 mm tested at 83 K was 24 % less than at room temperature. Regardless of stress triaxial value, tensile ductility at 83 K showed significant degradation. As above, there is a clear risk in using Mg alloys for structural materials at cryogenic temperatures.
2. In present study, three fracture behavior types were observed by SEM: (1) ductile fracture forming dimples in the smooth round bar specimen tested at room temperature, (2) rugged and intergranular fracture surfaces in notched round bar specimens tested at room temperature and (3) fracture surfaces at 83 K where coarse second phase particle fractures occur frequently, regardless of stress triaxiality. From this, coarse particle fracture strength under cryogenic temperature is assumed extremely low.
3. It is important to consider the scope and application of the Rice and Tracy model for fracture behavior in the AZ31Mg alloy at cryogenic temperatures, as different plastic deformation and fracture processes occur compared to room temperature.

Acknowledgments

This study was supported by the AMADA foundation (AF-2019025-B3) and the education and research project at Toyohashi University of Technology. The authors also appreciate the financial assistance of the Light Metal Educational Foundation, Japan.

REFERENCES

[1] B.L. Mordike and T. Ebert, "Magnesium Properties – Applications - Potential", *Mater. Sci. Eng. A., vol. 302, 37-145, 2001*
[2] J.W. Hancock and A.C. Mackenzie, "On the Mechanisms of Ductile Failure in High-Strength Steels subjected to Multi-Axial Stress-States", *J. Mech. Phys. Solids, vol. 24, 147-169, 1979*
[3] H. Li, M.W. Fu, J. Lu and H. Yang, "Ductile Fracture: Experiments and Computations", *Inter. J. Plasticity, vol.27, 147-180, 2011*
[4] I. Westermann, K. O. Pedersen, T. Furu, T. Børvik and O. S. Hopperstad, "Effects of Particles and Solutes on Strength, Work-Hardening, and Ductile Fracture of Aluminum Alloys", *Mech. Mater., vol. 79, 58-72, 2014*
[5] J. Peng, Y. Wang, Q. Dai, X. Liu and Z. Zhang, "Effects of Stress Triaxiality on Plastic Damage Evolution and Failure Mode for 316L Notched Specimen", *Metals, vol. 9, 1067, 2019*
[6] B. Kondori and A.A. Benzerga, "Effects of Stress Triaxiality on the Flow and Fracture of Mg Alloy AZ31", *Metall. Trans. A, vol. 45, 3292-3307, 2014*
[7] F.F. Li and G. Fang, "Stress-State Dependency of Ductile Fracture in an Extruded Magnesium Alloy and Its Underlying Mechanisms", *Inter. J. Plasticity, vol. 152, 103258, 2022*
[8] P.W. Bridgman, "Studies in Large Plastic Flow and Fracture", *First Edition, McGraw-Hill Company Inc., 1952*
[9] R. Zheng, W. Gong, J.P. Du, S. Gao, M. Liu, G. Li, T. Kawasaki, S. Harjo, C. Ma, S. Ogata and N. Tsuji, "Rediscovery of Hall-Pech Strengthening in Bulk Ultrafine Grained Pure Mg at Cryogenic Temperature: A Combined In-Situ Neutron Diffraction and Electron Microscopy Study", *Acta Matell., vol. 238, 118243, 2022*
[10] A. Takahashi, N. Yamamoto and T. Toyohiro, "Fundamental Study on Impact Toughness of Magnesium Alloy at Cryogenic Temperature", *Inter. J. Innovations Eng. Tech., Special Issue on ACEIAT & JTSTE – Thailand 2014, 1-14, 2015*
[11] F.A. McClintock, "A Criterion for Ductile Fracture by Growth of Hole", *J. Appl. Mech., vol. 35, 353-371, 1968*
[12] J.R. Rice and D.M. Tracy, "On the Ductile Enlargement of Voids in Triaxial Stress Fields", *J. Mech. Phys. Solids, vol. 17, 201-217, 1968*
[13] A.L. Gurson, "Continuum Theory of Ductile Rupture by Void Nucleation and Growth: Part I – Yield Criteria and Flow Rules for Porous Ductile Media", *J. Eng. Mater. Technol., vol. 99, 2-15, 1977*
[14] A. Needleman and V. Tvergaard, "An Analysis of Ductile Rupture in Notched Bars", *J. Mech. Phys. Solids, vol. 32, 461-490, 1984*
[15] V. Tvergaard and A. Needleman, "Analysis of the Cup-Cone Fracture in a Round Tensile Bar", *Acta Metall., vol. 32, 157-169, 1984*
[16] M. Gologanu, J.B. Leblond and J. Devaux, "Approximate Models for Ductile Metals Containing Nonspherical Voids – Case of Axisymmetric Prolate Ellipsoidal Cavities", *J. Mech. Phys. Solids, vol. 41, 1723-1754,1993*
[17] X. Gao, T. Wang and J. Kim, "On Ductile Fracture Initiation Toughness: Effect of Void Volume Fraction, Void Shape and Void Distribution", *Inter. J. Solids Struct., vol. 42, 5097-5117, 2005*
[18] P.F. Thomason, "A Three-Dimensional Model for Ductile Fracture by the Growth and Coalescence of Microvoids", *Acta Metall. Vol. 33, 1087-1095, 1985*
[19] T. Kobayashi, M. Niinomi and M. Adachi, "Effects of Triaxiality and Microstructure on the Ductile Fracture Morphology of Al-Zn-Mg-Cu-Zr Alloys, *J. Japan Inst. Metals, vol. 52, 26-33, 1988* (in Japanese)
[20] T. Kobayashi, M. Niinomi, T. Irisa, T. Sakai, T. Hagiwara and T. Sakamoto, "Effect of Stress Triaxiality on Fracture Behavior of 2091 Aluminum Alloys", *J. Japan Inst. Light Metals, vol. 45, 654-659, 1995* (in Japanese)
[21] T. Kobayashi, Y. Muranaka and S. Yamada, "Effects of Stress Triaxiality and Matrix Microstructure on Ductile Fracture in Ductile Cast Iron", *J. Japan Foundry Engineering Society, vol. 69, 924-929, 1997* (in Japanese)
[22] T. Masuda, M. Takada, H. Toda, T. Kobayashi and L. Wang, "Stress Triaxiality Effect on Dynamic Tensile Properties in a 6061-T6 Aluminum Alloy", *J. Japan Inst. Light Metals, vol. 54, 175-181, 2004* (in Japanese)